MedCrave
Step into the World of Research
Open Access Journal of Mathematical and Theoretical Physics

Research Article

Open Access
CrossMark

Theoretical treatment of cold penning ion source with axial extraction

Abstract

The present work investigates theoretical treatment of proposed design for high ion beam efficiency using cold Penning ion source with axial extraction. The derivation of the electric field at any point on the axis of symmetry of the source has been carried out. The electric field is given taking into consideration the effect of the anode radius cylinder, the length of the cylindrical anode and the distance between the center and any of the two flat earthed cathodes. Two different shapes of the electric field near the symmetrical axis have been deduced and the condition of producing an electrostatic confined discharge was obtained. A proposed design of cold Penning discharge ion source with axial extraction is obtained according to the theoretical treatment.

Keywords: cold cathode penning ion source, axial extraction, electric field distribution

Volume 1 Issue 3 - 2018

OA Mostafa, H El-Khabeary, Samah I Radwan
Accelerators and Ion Sources Department, Basic Nuclear Science Division, Egypt

Correspondence: H El-Khabeary, Accelerators and Ion Sources Department, Basic Nuclear Science Division, Nuclear Research Center, Atomic Energy Authority, P No.13759, Cairo, Egypt, Email helkhabeary@yahoo.co.uk

Received: March 27, 2018 | **Published:** May 24 2018

Introduction

The Penning ion source is one of the plasma ion sources that produce high voltage, low pressure plasma discharge between cold cathodes and the anode.[1–4] In the Penning ion source, a DC voltage in the range of 500 - 5000volts is applied between the anode and the cathode, while the two cathodes are at the same potential. The primary electrons oscillate along the axial direction between the two cathodes cause ionization by collision with the gas molecules.[4] Arrangement of the electrodes increases the efficiency of the discharge by increasing the path length of the ionizing electrons through the discharge region; the electric field distribution induced by the applied voltage forces the ionizing electrons to oscillate between the two cathodes.[5] The cylinderical anode must be made of high ionization coefficient material such as stainless steel, copper, carbon, etc., whilethe cathode material must have high secondary electrons emission coefficient as aluminium, magnesium and beryllium which yields an increase for the plasma density and therefore a higher ion current can be produced.

The ions can be extracted either axially through one cathode in the direction parallel to the discharge axis or, more commonly, radially through a slit in the anode normal to the discharge axis direction.[6,7]

The cold cathode Penning ion source is more successful than other sources for many types of accelerators.[8,9] It is characterised by simple design, comapct in size, maintenance free, long time of operation with no filament and operates at low pressure and can be used for different applications such as production of multicharged ions from heavy gaseous atoms,[10] sputtering,[11] materials surface modification,[12] ion implantation and thin films deposition of different materials.[13]

Theoretical analysis

Consider a cylindrical electrode with inner radius, a, and length, 2h, is placed between two electrodes such that the distance between the center of the cylinder and any of the two plane electrodes is, d, as shown in Figure 1A. Assume a charge of density ρ is produced on the inner surface of the cylinder due to applied potential, V, on it. The electric field intensity and potential at any point on the symmetrical axis, Z, can be obtained by applying the image theory.[14] Figure 1B shows a cylindrical electrode of charge density ρ which has two images of $-\rho$ charge density at the two sides of the cylindrical electrode, such that the center of any image is at distance equal to 2d from the cylindrical electrode center.

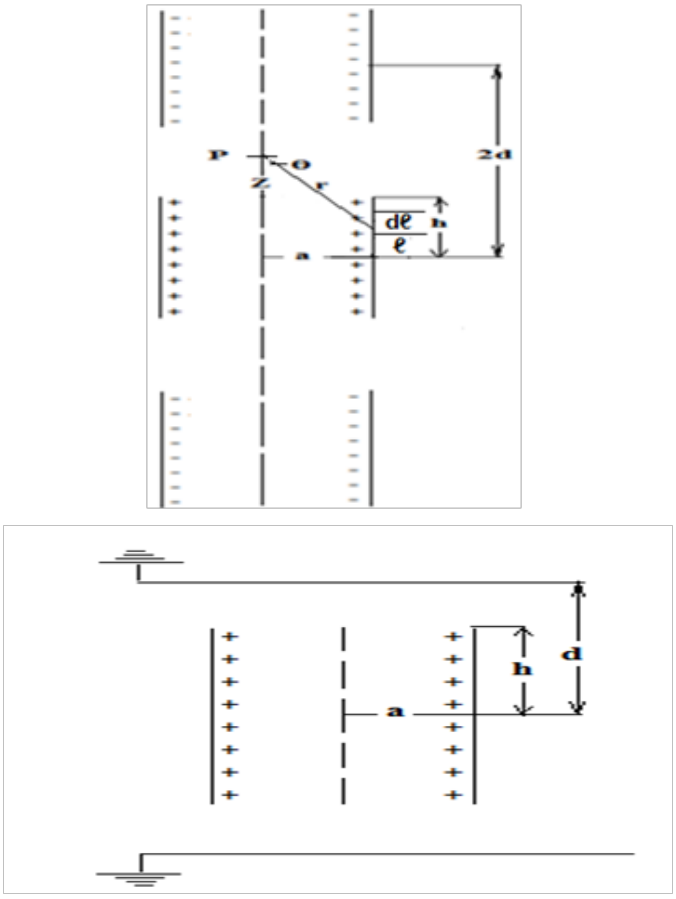

Figure 1 Determination of the electric field using image theory.

Electric field intensity at point P on the axis of symmetry

The electric field intensity, ΔE, at a point P on the axis of symmetry at a distance Z from the cylinder center due to an elementary area,

© 2018 Mostafa et al. This is an open access article distributed under the terms of the Creative Commons Attribution License, which permits unrestricted use, distribution, and build upon your work non-commercially.

Copyright: ©2018 Mostafa et al.

ΔA, of the original cylinder in the form of a sector of radius, a, and length, dl, is given by:

$$\Delta E=\frac{\rho\Delta A}{4\pi\in_o r^2}\cos\theta \qquad (1)$$

Where $\in_o$ is the permitivity of the medium.

$$\Delta E=\rho\frac{2\pi\ a\ dl}{4\pi\in_o r^2}\frac{(Z-l)}{r}=\frac{\rho\ a}{2\in_o}\frac{(Z-l)}{r^3}dl \qquad (2)$$

Since $r=\sqrt{a^2+(Z-l)^2}$

Therefore $r=\sqrt{a^2+(Z-l)^2}$

Consequently $r^3=[a^2+(Z-l)^2]^{3/2}$ (3)

Substituting equation (3) in equation (2) gives:

$$\Delta E=\frac{\rho a}{2\in_o}\frac{(Z-l)}{[a^2+(Z-l)^2]^{3/2}}dl$$

Therefore, the electric field intensity at P is:

$$E_1=\int_{-h}^{h}\Delta E=\frac{\rho\ a}{2\in_o}\left[\frac{1}{\sqrt{a^2+(Z-h)^2}}-\frac{1}{\sqrt{a^2+(Z+h)^2}}\right] \qquad (4)$$

The electric field Intensity due to the upper cylinder of density $-\rho$ as shown in Figure 1B can be obtained by putting (2d-Z) instead of Z in equation (4) then

$$E_2=\frac{\rho a}{2\in_o}\left[\frac{1}{\sqrt{a^2+(2d-Z-h)^2}}-\frac{1}{\sqrt{a^2+(2d-Z+h)^2}}\right] \qquad (5)$$

The electric field intensity due to the lower cylinder of charge density $-\rho$ as shown in Figure 1B can be obtained by putting (2d+Z) instead of Z and $-\rho$ instead of ρ in equation (4) then

$$E_3=\frac{-\rho a}{2\in_o}\left[\frac{1}{\sqrt{a^2+(2d+Z-h)^2}}-\frac{1}{\sqrt{a^2+(2d+Z+h)^2}}\right] \qquad (6)$$

so, the total electric field at point P is:

$$E=E_1+E_2+E_3=\frac{\rho a}{2\in_o}\left[\left\{\frac{1}{\sqrt{a^2+(Z-h)^2}}-\frac{1}{\sqrt{a^2+(Z+h)^2}}\right\}+\left\{\frac{1}{\sqrt{a^2+(2d-Z-h)^2}}-\frac{1}{\sqrt{a^2+(2d-Z+h)^2}}\right\}-\left\{\frac{1}{\sqrt{a^2+(2d+Z-h)^2}}-\frac{1}{\sqrt{a^2+(2d+Z+h)^2}}\right\}\right] \qquad (7)$$

Total potential at point P on the axis of symmetry

The potential ΔV due to an elementary area ΔA of the original cylinder of charge density ρ will be:

$$\Delta V=\frac{\rho.\Delta A}{4\pi\in_o r}$$

$$\Delta V=\frac{\rho.2\pi a.dl}{4\pi\in_o r}=\frac{\rho a}{2\in_o}\frac{dl}{\sqrt{a^2+(Z-l)^2}}=\frac{\rho a}{2\in_o}\frac{dl}{\sqrt{l^2-2Zl+\left(a^2+Z^2\right)}}$$

Therefore, the potential at P is:

$$V_1=\int_{-h}^{h}\Delta V=\frac{\rho a}{2\in_o}\ln\left[\frac{2h-2Z+2\sqrt{h^2+a^2-2Zh+Z^2}}{-2h-2Z+2\sqrt{h^2+a^2+2Zh+Z^2}}\right] \qquad (8)$$

The potential due to the upper cylinder of charge density, $-\rho$ can be obtained by putting (2d-Z) and $(-\rho)$ instead of (Z) and (ρ) respectively in equation (8). Therefore, the potential will be:

$$V_2=\frac{-\rho a}{2\in_o}\ln\left[\frac{2h-2(2d-Z)+2\sqrt{h^2+a^2-2h(2d-Z)+(2d-Z)^2}}{-2h-2(2d-Z)+2\sqrt{h^2+a^2+2h(2d-Z)+(2d-Z)^2}}\right] \qquad (9)$$

The potential due to the lower cylinder of charge density, $-\rho$, can be obtained by putting (2d+Z) and $(-\rho)$ instead of (Z) and (ρ) respectively in equation (8). Therefore, the potential will be:

$$V_3=\frac{-\rho a}{2\in_o}\ln\left[\frac{2h-2(2d+Z)+2\sqrt{h^2+a^2-2h(2d+Z)+(2d+Z)^2}}{-2h-2(2d+Z)+2\sqrt{h^2+a^2+2h(2d+Z)+(2d+Z)^2}}\right] \qquad (10)$$

So, the total potential, V_T, at a point P will be:

$$V_T=V_1+V_2+V_3$$

By substituting Z = 0 in equations (8), (9) and (10) and finding V_T which is equal to the potential of original cylinder V

$$V=\frac{\rho a}{2\varepsilon_o}\left[\ln\left\{\frac{2h+2\sqrt{a^2+h^2}}{-2h+2\sqrt{a^2+h^2}}\right\}-2\ln\left\{\frac{2h-4d+2\sqrt{h^2+a^2-4hd+4d^2}}{-2h-4d+2\sqrt{h^2+a^2+4hd+4d^2}}\right\}\right]$$

Therefore

$$\frac{\rho a}{2\varepsilon_o}=\frac{V}{\ln\left\{\frac{2h+2\sqrt{a^2+h^2}}{-2h+2\sqrt{a^2+h^2}}\right\}-2\ln\left\{\frac{2h-4d+2\sqrt{h^2+a^2-4hd+4d^2}}{-2h-4d+2\sqrt{h^2+a^2+4hd+4d^2}}\right\}} \qquad (11)$$

By substituting $\frac{\rho a}{2\varepsilon_o}$ of equation (11) in equation (7) then E can be obtained in terms of V, a, h and d.

Results and discussion

Figures 2-5 show the distribution of $(E/V).a$ along the symmetrical axis for different values of h at d / a equal to 1.5, 2, 2.5 and 3 respectively. Each of these distribution is characterized by a maximum value exists between the center of the source and any of the two earthed plane electrodes for $h/a < 0.4$, $h/a < 1.2$, $h/a < 2$ and $h/a < 2.4$ at d / a equal to 1.5, 2, 2.5 and 3 respectively. It is clear in this case that the field near the symmetrical axis has a saddle configuration. The maximum value of $(E/V).a$ only exists at any of the plane earthed cathodes when $h/a \geq 0.4$, $h/a \geq 1.2$, $h/a \geq 2$ and $h/a \geq 2.4$ at d / a equal to 1.5, 2, 2.5 and 3 respectively. This maximum value of $(E/V).a$ increases by increasing h. Hence the field is a convergent type and its degree of convergence increases by increasing h.

Figure 6 shows the two-different d - h domains from d/a = 1.5 to d/a = 3 for saddle field and convergent field types. Figure 7 represents the relation of $\Delta[(E/V).a]$, difference of $(E/V).a$ between the center of the source and any of the two plane earthed cathodes, and d/a for h

Citation: Mostafa OA, El-Khabeary H, Radwan SI. Theoretical treatment of cold penning ion source with axial extraction. *Open Acc J Math Theor Phy.* 2018;1(3):102–105. DOI: 10.15406/oajmtp.2018.01.00015

Copyright:
©2018 Mostafa et al.

= 0.8d which lies in the convergent field domain of Figure 6. It is clear that the degree of convergence increases by decreasing d from 3 to 1.5. Accordingly, proposed design of the source for good confinement by choosing, d/a = 1.5 and h = 0.8d. The value of cylinder radius, a, may be chosen equal to 2 cm.

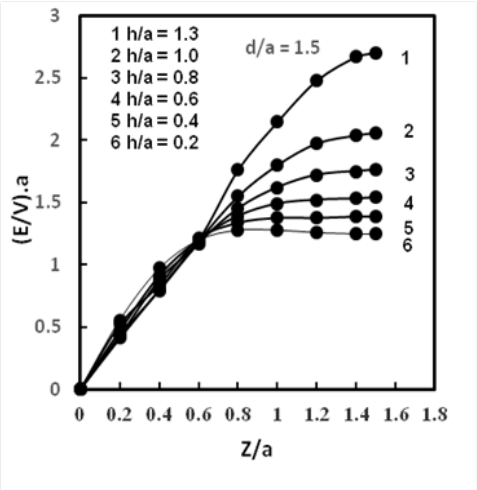

Figure 2 The distribution of (E/V).a along the symmetrical axis at different values of h for d/a=1.5.

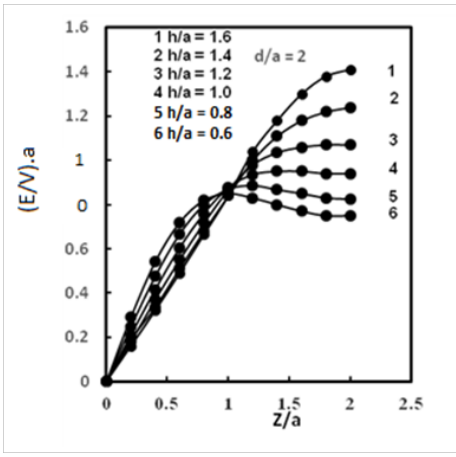

Figure 3 The distribution of (E/V).a along the symmetrical axis at different values of h for d/a=2.

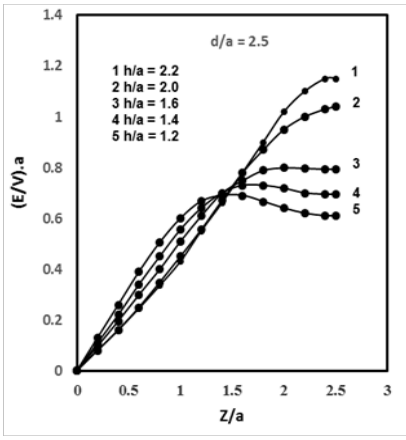

Figure 4 The distribution of (E/V).a along the symmetrical axis at different values of h for d/a=2.5.

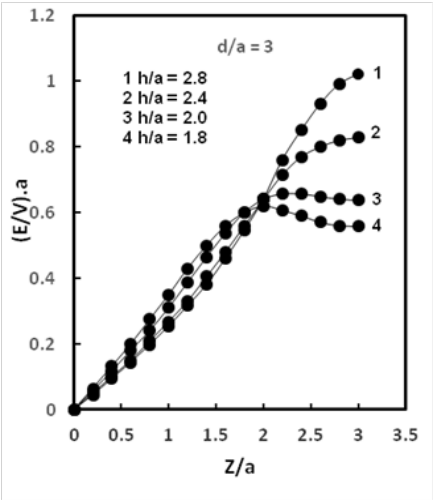

Figure 5 The distribution of (E/V).a along the symmetrical axis at different values of h for d/a=3.

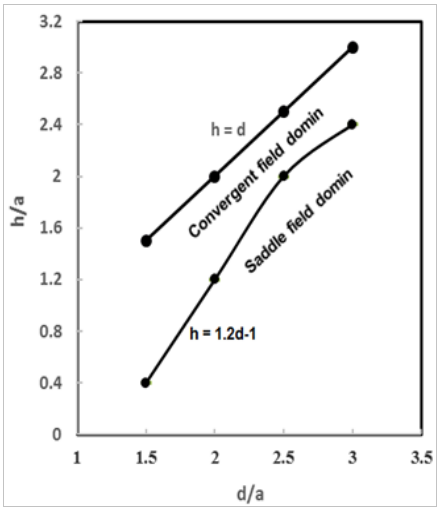

Figure 6 Different d - h domains for different field types.

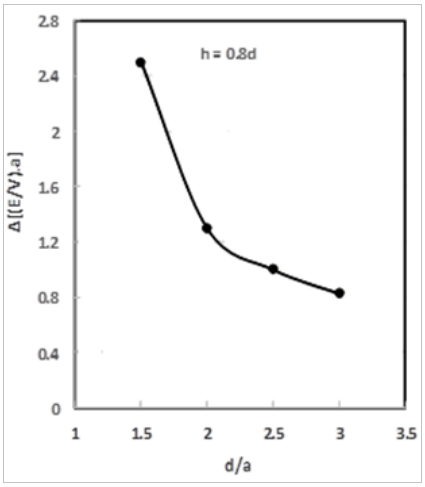

Figure 7 Δ(E/V).a versus d/a for h=0.8d.

Citation: Mostafa OA, El-Khabeary H, Radwan SI. Theoretical treatment of cold penning ion source with axial extraction. *Open Acc J Math Theor Phy.* 2018;1(3):102–105. DOI: 10.15406/oajmtp.2018.01.00015

Copyright: ©2018 Mostafa et al.

Conclusion

The theoretical analysis of the electric field distribution shows two different shapes, convergent field and saddle field, depending on the source parameters. The domains h–d is obtained for such field shapes, assuming positive polarity on the cylindrical electrode and two plane earthed cathodes. Convergent field type of such polarity confine the discharge at the two plane earthed cathodes such that an ion source of high ion beam efficiency is available. Proposed design optimum dimensions of such source for good confinement are d/a=1.5, h=0.8d and the radius of the cylinder, a, may be chosen equal to 2cm.

Acknowledgements

None.

Conflict of interest

The authors declare that there is no conflict of interest.

References

1. Rovey JL, Ruzic BP, Houlahan TJ. Simple Penning ion source for laboratory research and development applications. *Review of Scientific Instruments*. 2007;78:106101.
2. Rovey JL. Design parameter investigation of a cold-cathode Penning ion source for general laboratory applications. *Plasma Sources Science and Technology*. 2008;17(3).
3. Das BK, Shyam A, Das R, et al. Development of hollow anode penning ion source for laboratory application. *Nuclear Instruments and Methods in Physics Research A*. 2012;669:19–21.
4. Brown IG. The Physics and Technology of Ion Sources. New York: Wiley; 2004. 396 p.
5. Sy AV. Nuclear Engineering. Berkeley; California University; 2013.
6. Abdelrahman MM, Zakhary SG. Simulation studies for ion beam extraction systems. *Brazilian J Phys*. 2009;39(2):275–279.
7. Giannuzzi LA, Stevie FA. Introduction to Focused Ion Beams. USA: Springer; 2005.
8. Abdel Rahman MM. Ion Sources for Use in Research and Low Energy Accelerators. *International Journal of Instrumentation Science*. 2012;1(5):63–77.
9. Abdelbaki MM, Abdelrahman MM, Basal NI. D.C. cold cathode penning ion source for low energy accelerator. *Radiation Physics and Chemistry*. 1996;47(5):669–671.
10. Cun H, Spescha A, Schuler A, et al. Characterization of a cold cathode Penning ion source for the implantation of noble gases beneath 2D monolayers on metals: Ions and neutrals. Journal of Vacuum Science & Technology A: Vacuum, Surfaces, and Films. 2016;34(2).
11. Nouria Z, Lib R, Holta RA, et al. A Penning sputter ion source with very low energy spread. *Nuclear Instruments and Methods in Physics Research Section A*. 2010;614(2):174–178.
12. Das BK, Das R, Shyam A. Solid State Physics, Proceedings of The 55th Dae Solid State Physics Symposium 2010. AIP Conference Proceedings. 2011;1349(1):447–448.
13. Manova D, Gerlach JW, Mandl S. Thin Film Deposition Using Energetic Ions. *Materials*. 2010;3(8):4109–4141.
14. Ramsey S. Electricity and Magnetism: An introduction to the mathematical theory. Cambridge University Press. 1st ed. 2009; 284 p.